

Heavy Flavour Measurements in pp and Pb–Pb Collisions with the ALICE Experiment at LHC

C. Zampolli* for the ALICE Collaboration

December 3, 2021

Abstract

Heavy flavour is mainly produced during the initial hard partonic interactions in a heavy ion collision, and is well-suited to probe the early phases of the evolution of the system. This contribution will focus on Pb–Pb analyses at a centre-of-mass energy per nucleon pair of 2.76 TeV, with some hints at the pp data at 7 and 2.76 TeV. Results of open heavy flavour analyses will be shown for various decay channels, including electrons, muons, and hadronic charm decays, together with results obtained for heavy quarkonia at both central and forward rapidities.

1 Introduction

The extreme energy density and temperature conditions reached in Pb–Pb collisions at LHC energies are expected to generate a deconfined plasma of quarks and gluons (the so-called Quark-Gluon Plasma, QGP [1]), from which a phase transition to ordinary colourless hadronic matter takes place as a consequence of subsequent expansion and cooling down. Among the various observables that shed light on the properties of the QGP, heavy flavour production is expected to provide unique and important probes. Since heavy quarks (charm and beauty) are produced during the early stages of the collisions, they experience the whole evolution of the system. High momentum open charm and beauty are of great interest for the role they play in the study of the in-medium partonic energy loss. Such energy loss occurs due to elastic processes (collisional energy loss) [2], as well as inelastic processes [3, 4] that are expected to dominate at high momentum. Due to the smaller QCD colour coupling (Casimir factor) for quarks than for gluons, the energy loss expected for quarks should be smaller than that for gluons. Since light flavour hadrons arise dominantly from gluon jets, this effect may exhibit itself in different suppression patterns for light and heavy flavour hadrons. Moreover the “dead cone effect” should reduce the radiation at small angles for heavy quarks, imposing a further hierarchy on the energy loss depending on the mass of the quark [5].

The study of quarkonium can provide important insight on the properties of the medium. Production of charmonium in a QGP is determined by the mechanism of colour screening [6], which leads to a suppressed production in a hot medium compared to pp collisions. Moreover, the abundant production of

*INFN Sezione di Bologna, Chiara.Zampolli@cern.ch

charm quark pairs at LHC energies could lead to a new mechanism of charmonium formation via recombination of uncorrelated charm-anticharm quarks in a deconfined medium [7, 8], which could even result (depending on the overall charm abundance) in a J/ψ production in Pb–Pb enhanced with respect to pp collisions.

Heavy quarks at the LHC are an important probe also in pp collisions. Such measurements enable tests of theoretical calculations based on perturbative QCD for heavy quark production in a new energy regime. They could shed light on the hadroproduction mechanisms that govern quarkonia production. This is an important outstanding problem, since current theoretical models cannot satisfactorily describe measurements of heavy quark rapidity and p_t distributions, and polarization. pp data also provide an essential baseline for Pb–Pb measurements, the comparison with which is needed to discriminate between initial and final effects in their production.

Figure 1 shows the total charm-anticharm cross section in the full phase space as a function of the centre-of-mass for different experiments ([9] and references therein). The ALICE values refer to the measurements at $\sqrt{s} = 2.76$ and 7 TeV and were extrapolated down to $p_t = 0$ and at full rapidity using FONLL calculations. The LHCb [10] and ATLAS [11] points are drawn as well. As one can see, the values at the LHC are ~ 10 times larger than those at RHIC, making the LHC a “heavy flavour factory”.

The paper is organized as follows. First, a brief description of the ALICE experiment will be given in Section 2 focusing on the detectors involved in the heavy flavour studies. In Sec. 3 the results for the open heavy flavour analyses will be presented. These include the open charm mesons in the decay channels $D^0 \rightarrow K^- \pi^+$, $D^+ \rightarrow K^- \pi^+ \pi^+$ and $D^{*+} \rightarrow D^0 \pi^+$, and the analysis of the semi-electronic decays $D, B \rightarrow e + X$ at midrapidity (more details can be found in [16]), together with the study of the heavy flavour muons at forward rapidity (see also [17]). The results for the J/ψ analysis in the electronic and muonic decay channel, at central and forward rapidity respectively, will be presented in Sec. 4 (for more details see also [18]). Finally, some concluding remarks will be given in Sec. 5.

2 The ALICE experiment and its heavy flavour program

ALICE [19] is the experiment at the Large Hadron Collider (LHC) devoted to the study of ultra-relativistic heavy-ion collisions. The ALICE heavy flavour program relies on the excellent tracking and particle identification capabilities of the experiment. In the ALICE central barrel, covering the pseudorapidity range $|\eta| < 0.9$, in a magnetic field of 0.5 T, the Inner Tracking System (ITS) and the Time Projection Chamber (TPC) are the main tracking devices. The ITS is primarily dedicated to the reconstruction of the primary and secondary vertices, with a transverse impact parameter resolution better than $75 \mu\text{m}$ for $p_t > 1 \text{ GeV}/c$. The two innermost layers of the ITS, the Silicon Pixel Detector (SPD), are also used to provide the minimum-bias trigger to the experiment together with the VZERO detector¹. Besides tracking and momentum determination, the

¹The ALICE VZERO detector, covering the pseudorapidity regions $2.8 < \eta < 5.1$ and $-3.7 < \eta < -1.7$, is made up of two arrays of scintillator tiles on both sides of the interaction point, and is aimed at providing the minimum-bias trigger, and centrality and luminosity

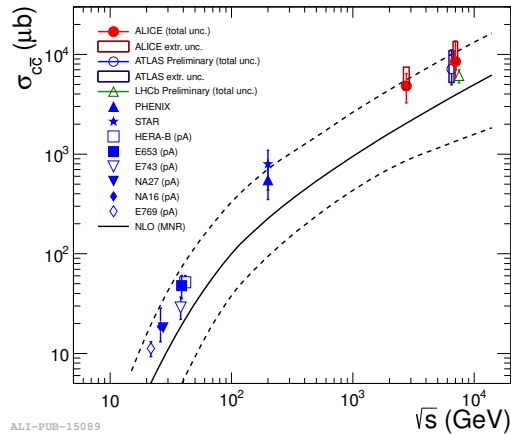


Figure 1: Charm-anticharm cross section for the full p_t and rapidity phase space as a function of the centre-of-mass energy for different experiments at HERA, FNAL, SPS, RHIC and the LHC, for different collisions systems (pp collisions for the LHC points) [9–14]. The LHCb and ATLAS measurements are slightly shifted for visibility. The NLO MNR calculation is also drawn [15].

TPC is used in the heavy flavour analyses also for particle identification (PID) of charged particles via specific energy deposition dE/dx . Charged hadrons at intermediate momenta are identified by the ALICE Time Of Flight (TOF) detector. Electron PID is carried out for $p_t < 4$ GeV/ c by the TPC and the TOF detectors, while in the range $p_t > 1$ GeV/ c the Transition Radiation Detector (TRD) is used. The Electromagnetic Calorimeter (EMCAL) identifies electrons at high momenta ($p_t > 5$ GeV/ c). Finally, the ALICE Muon Spectrometer at $-4 < \eta < -2.5$ performs both the reconstruction and the identification of muon tracks with $p_t > 4$ GeV/ c .

3 Open heavy flavour

In this section, the main ALICE open heavy flavour analyses will be discussed. The results included here will cover both data collected in pp collisions at $\sqrt{s} = 7$ TeV and Pb–Pb collisions at $\sqrt{s_{NN}} = 2.76$ TeV. Emphasis will be put on the nuclear modification factor R_{AA} defined as:

$$R_{AA}(p_t) = \frac{d^2 N^{AA}/d\eta dp_t}{\langle T_{AA} \rangle d^2 \sigma^{pp}/d\eta dp_t} \quad (1)$$

Here, $\langle T_{AA} \rangle$ is the average nuclear overlap function for a given centrality class and is proportional to $\langle N_{coll} \rangle$. R_{AA} quantifies the effect of the hot and dense medium created in heavy-ion collisions by comparing the production yield in pp collisions, after an appropriate scaling via the number of binary collisions, to that obtained in Pb–Pb interactions. Any observed deviation of R_{AA} from unity is due to effects specific to nuclear collisions.

information.

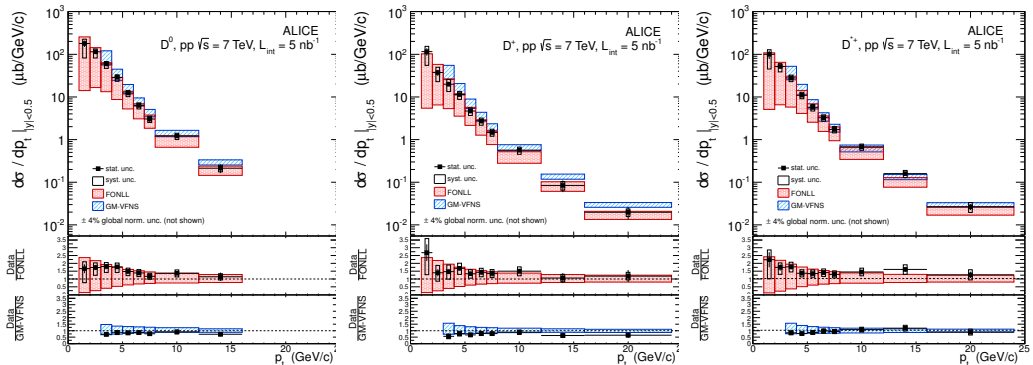


Figure 2: D^0 (left), D^+ (middle), and D^{*+} (right) inclusive cross sections as a function of p_t measured by ALICE in pp collisions at $\sqrt{s} = 7$ TeV [20].

3.1 D mesons

The hadronic decay channels $D^0 \rightarrow K^-\pi^+$, $D^+ \rightarrow K^-\pi^+\pi^+$, and $D^{*+} \rightarrow D^0\pi^+$ were used for the study of open charm production. The analysis of these channels is based on the topology of the decay, characterized by a secondary vertex displaced from the primary one, and exploits the excellent vertex reconstruction and tracking capabilities of the ALICE ITS and TPC detectors. The background is reduced at low transverse momenta by combining the TPC and TOF PID information. In order to minimize as much as possible the signal loss due to the usage of the PID, the rejected candidates are those for which the daughters have been identified by both TPC and TOF, but the two detectors provide different PID responses. In addition to such cases, also candidates for which the two daughter tracks were both identified as pions or as kaons were discarded.

Figure 2 [20] shows the D^0 , D^+ and D^{*+} p_t -differential inclusive cross sections in $|y| < 0.5$, obtained from pp events at $\sqrt{s} = 7$ TeV. Efficiency and acceptance corrections were applied to the raw data, after the B feed-down correction was estimated using FONLL predictions and applied [21]. In this figure (as well as in the following figures, unless specified otherwise), the error bars refer to statistical uncertainties, while boxes correspond to systematic uncertainties. The measured cross sections are found to be well described within uncertainties by the predictions from the FONLL and GM-VFNS calculations, based on perturbative QCD [21, 22]. For more details on the analysis see [20].

In the case of Pb–Pb data, the D meson spectra as a function of p_t and in different centrality bins² are obtained following the same procedure [25]. These spectra are then compared to those obtained in pp collisions. The comparison can be carried out if the pp data were taken at the same energy, and after rescaling them by $\langle T_{AA} \rangle$ via R_{AA} (Eq. 1). Due to the limited statistics of the pp data sample collected at $\sqrt{s} = 2.76$ TeV, which results in a limited precision and p_t coverage, the pp reference spectra were obtained by using a \sqrt{s} -scaling of the cross sections measured at $\sqrt{s} = 7$ TeV (see [25] for more details). The results for R_{AA} of prompt D^0 , D^+ and D^{*+} mesons are shown in

²The centrality of the collision is defined in terms of percentiles of the hadronic Pb–Pb cross section and determined from the distribution of the summed amplitudes in the VZERO scintillator tiles. This is fitted according to the Glauber model [23] to describe the collision geometry [24].

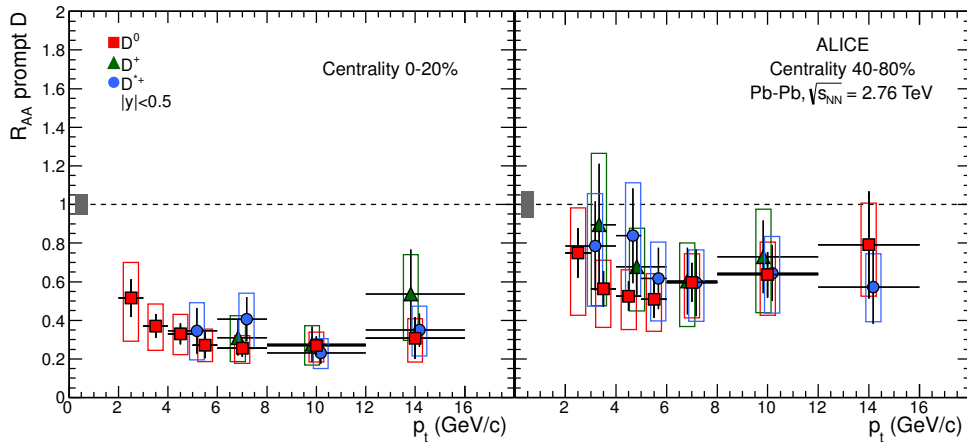


Figure 3: ALICE prompt D^0 , D^+ , and D^{*+} R_{AA} as a function of p_t in two different centrality classes: the left panel corresponds to 0–20% (central) events, while the right panel shows the results for 40–80% (semiperipheral) events [25].

Fig. 3 for the central (0–20% centrality class) and semi-peripheral (40–80%) events. R_{AA} for the three species agree with each other in both centrality classes and over the p_t ranges where they are measured (i.e. $2 \leq p_t \leq 16$ GeV/c, $6 \leq p_t \leq 16$ GeV/c, $5 \leq p_t \leq 16$ GeV/c, for D^0 , D^+ and D^{*+} in the 0–20% centrality class, and $2 \leq p_t \leq 16$ GeV/c, $3 \leq p_t \leq 12$ GeV/c, $2 \leq p_t \leq 16$ GeV/c, for D^0 , D^+ and D^{*+} in the 40–80% centrality class). Moreover, a clear increase in the R_{AA} is visible for more peripheral collisions, suggesting that in more central events initial state effects are more pronounced. A comparison of the averaged D meson R_{AA} with the charged hadrons R_{AA} was carried out. Since at high p_t ($p_t > 5$ GeV/c) it was shown that the charged hadron R_{AA} coincides with that for charged pions [26], the comparison would allow to test the prediction about the colour charge and mass dependence of energy loss, according to which heavy flavour should lose less energy than gluons, translating into $R_{AA}^D > R_{AA}^{charged}$. The results show quite good agreement between the heavy and light hadrons R_{AA} especially at $p_t \sim 5$ GeV/c. Nevertheless, there are some indications that R_{AA}^D may be higher than $R_{AA}^{charged}$ at low p_t (up to $\sim 30\%$ at 3 GeV/c). However, this observation is not at present conclusive, due to the limited statistical precision of the current data..

Comparisons with different theoretical models have also been carried out. Several models describe reasonably well both the charm R_{AA} and the light flavour R_{AA} . For more details on the analysis, see [25].

Another ongoing analysis of D mesons addresses the study of elliptic flow. Details and results from this analysis can be found in [16].

3.2 Electrons from heavy flavour decays

Heavy flavour production cross sections can be studied through the semielectronic decays of open charm and open beauty. The key tool for this analysis is the excellent electron PID capability of the ALICE experiment. The TPC dE/dx measurements together with the TOF information enable the identification of electrons in the low and intermediate p_t region (up to ~ 4 GeV/c).

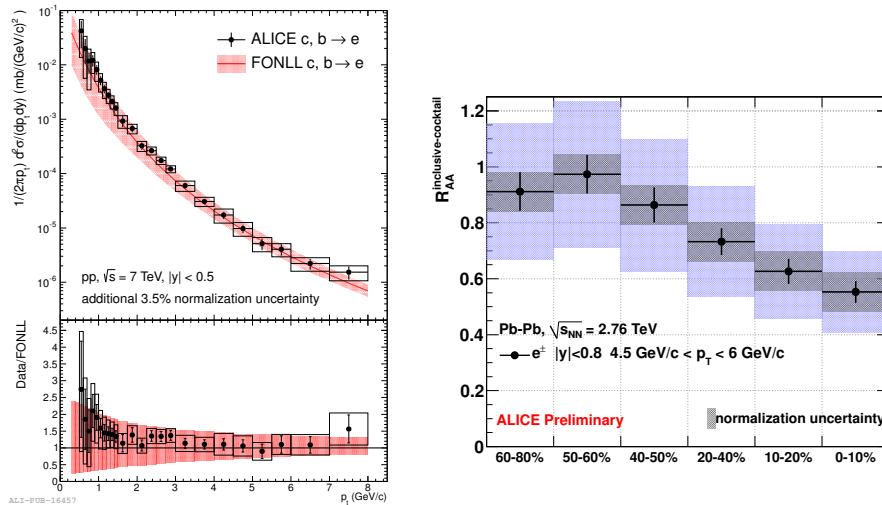


Figure 4: Left: p_t distribution for electrons from heavy flavour measured by ALICE in pp collisions at $\sqrt{s} = 7$ TeV. Superimposed are the predictions from FONLL calculations, the ratio to which is presented in the lower panel. Right: R_{AA} as a function of centrality for background subtracted electrons.

The analysis includes (at present only for pp data) also the TRD detector to suppress the π background. The EMCAL detector will be also added soon, in order to extend the p_t coverage of the measurements.

The inclusive electron p_t distributions of heavy-flavour decay electrons presented here for both pp and Pb–Pb collision data was obtained by subtracting from the inclusive electron spectrum a cocktail of the measured background sources of electrons, i.e. electrons from light hadron Dalitz decays (π^0 , ρ , ω , η), photon conversions in the material, heavy quarkonia (J/ψ and Υ), and direct radiation. The left panel of Fig. 4 shows the p_t spectrum obtained in pp collisions at $\sqrt{s} = 7$ TeV. The result from the cocktail analysis that allows to single out electrons from charm and beauty decays is presented. The distribution is compared to FONLL calculations, with which good agreement can be observed.

The same analysis approach was used in the case of Pb–Pb data at $\sqrt{s_{NN}} = 2.76$ TeV. In this case, the p_t distributions were obtained with the cocktail approach as a function of p_t and centrality. It was found that in central collisions a residual background at low p_t remained after the subtraction of the cocktail. This background is larger for more central collisions, possibly due to the contribution of thermal photons that are not included in the background removal. For each centrality class, the R_{AA} of background subtracted electrons is determined by taking as a reference the pp results at $\sqrt{s} = 7$ TeV, scaled to $\sqrt{s} = 2.76$ TeV using FONLL calculations, and scaling the ratio by $\langle T_{AA} \rangle$. It was found that in peripheral collisions the value of R_{AA} is compatible with one over the full p_t range measured (i.e. $1.5 < p_t < 6$ GeV/c), suggesting the absence of medium effects. On the contrary, a suppression can be seen increasing with centrality in the high p_t interval ($3.5 < p_t < 6$ GeV/c) where the charm and beauty decay contribution should dominate the electron spectrum according to the comparison between the inclusive electron spectrum and the cocktail. The R_{AA} measured as a function of centrality is reported in the right panel of Fig. 4,

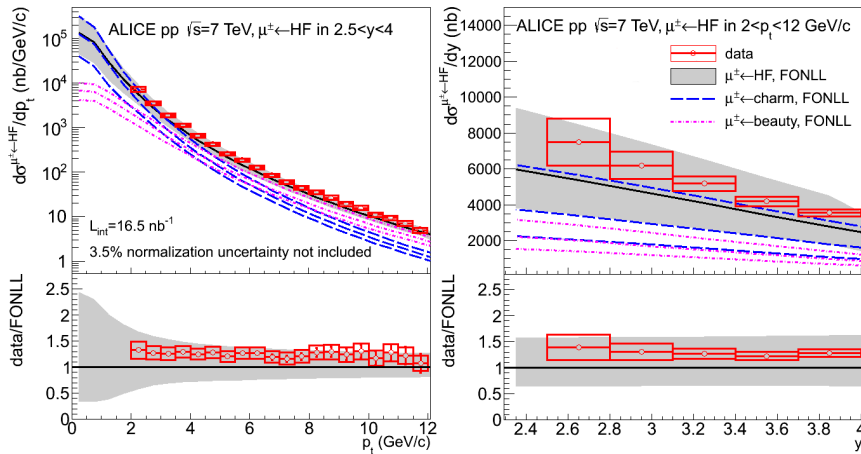


Figure 5: p_t (left) and y (right) differential inclusive cross section for muons from heavy flavour decays measured in pp collisions at $\sqrt{s} = 7$ TeV. Also shown are the predictions from FONLL calculations, considering the contributions from charm and bottom both together and separately [28].

integrating over the momentum range $4.5 < p_t < 6$ GeV/ c . As one can see the R_{AA} decreases from $\sim 0.9 \div 1$ to ~ 0.55 going from peripheral to central collisions, consistent with heavy flavour meson suppression due to partonic energy loss in the hot and dense medium created in central events. For more details see [27].

3.3 Muons from heavy flavour decays

Another important channel for the study of heavy flavour production is the semimuonic decay of charm and beauty. Muons coming from heavy flavour decays are reconstructed using the MUON spectrometer of ALICE. The MUON spectrometer, with both triggering and tracking chambers, covers the pseudorapidity region $-4 < \eta < -2.5$ and detects muons with momentum larger than 4 GeV/ c . The analysis strategy relies on event and track selection with subsequent subtraction of the background due to light hadrons (especially π and K from primary and secondary decays). The background subtraction is carried out using Monte Carlo simulations. For more details on the analysis strategy, see [28].

Figure 5 shows the p_t (left panel) and the rapidity (right panel) differential cross section for the reconstructed muons after background subtraction, efficiency and acceptance correction, obtained for pp data at $\sqrt{s} = 7$ TeV. The comparison with theoretical calculations from FONLL are also reported. There is in general good agreement with the predictions for both the p_t and the y distributions. The measured data lie above the central values of the FONLL calculation, but within the systematic uncertainties.

In order to extract the p_t distributions for heavy flavour muons in Pb–Pb collisions at $\sqrt{s_{NN}} = 2.76$ TeV, the same strategy was used. In this case, however, the background from light hadrons was not subtracted. It is estimated to be of the order of 6 – 15% (2 – 9%) for $p_t > 4$ GeV/ c ($p_t > 6$ GeV/ c) in central and peripheral collisions. This values were obtained from a minimum

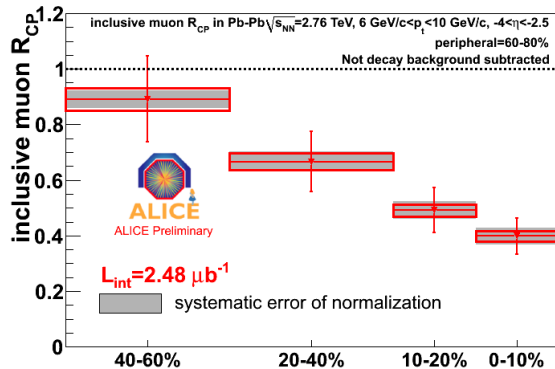


Figure 6: Inclusive R_{CP} for heavy flavour muons measured in Pb–Pb collisions at $\sqrt{s_{NN}} = 2.76$ TeV. The reference centrality is the 60 – 80% class.

bias simulation based on the HIJING generator [29] (without quenching).

The ratio of inclusive muons in central to peripheral events is defined as:

$$R_{CP}(p_t) = \frac{[1/\langle T_{AA} \rangle \times dN/dp_t]_{central}}{[1/\langle T_{AA} \rangle \times dN/dp_t]_{peripheral(60-80\%)}}$$

The Inclusive R_{CP} for heavy flavour muons is shown in Fig. 6. Here only muons with $p_t > 6$ GeV/c are considered in order to keep the background under control. As one can see, the suppression with respect to peripheral collisions becomes larger as centrality increases, from ~ 0.9 for the most peripheral to ~ 0.4 for the most central events. This could be interpreted as a consequence of the formation of a hot and dense medium in central events. For more details see also [30].

4 Quarkonia

In this section, some of the J/ψ measurements performed with the ALICE detector will be described, both from the analysis of the pp data at $\sqrt{s} = 7$ TeV and 2.76 TeV, and from the Pb–Pb data sample collected at $\sqrt{s_{NN}} = 2.76$ TeV. The nuclear modification factor R_{AA} will be presented. The measurements are carried out for the dielectron decay channel at midrapidity ($|y| < 0.9$), and the dimuon channel at forward rapidity ($-4 < y < -2.5$). For more details about the ALICE J/ψ results, refer to [31–35].

The J/ψ analysis at central rapidity relies on the PID information provided by the TPC detector. In future the analysis will include the TRD, TOF and EMCAL to improve the electron PID and the triggering capabilities. The signal extraction was performed via bin counting in the invariant mass range $2.92 < M_{inv} < 3.16$ GeV/c², with background removal performed by subtracting from the opposite-sign electron pairs' invariant mass distribution the corresponding like-sign distribution. The inclusive p_t -integrated cross section measured in pp collisions at 7 TeV is shown in the left panel of Fig. 7, together with the results for pp collisions at $\sqrt{s} = 2.76$ TeV (see [35] for more details).

In the same figure, the results from the J/ψ analysis at forward rapidity, i.e. $-4 < y < -2.5$, are included. In this rapidity interval, the measurement was

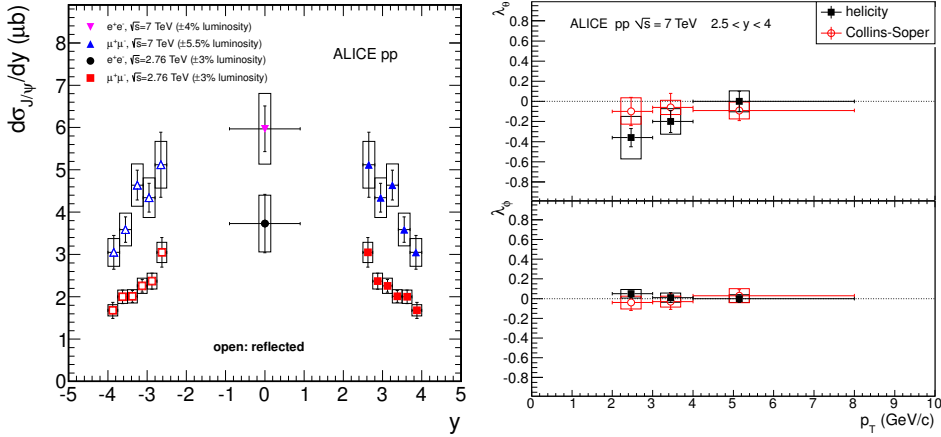


Figure 7: Left: inclusive p_t -integrated J/ψ cross section measured in pp collisions at 7 TeV. The results include the measurement at midrapidity and at forward rapidity. The measurement at $\sqrt{s} = 2.76$ are shown [35]. Right: λ_θ and λ_ϕ J/ψ polarization parameters as a function of p_t obtained in pp collisions at $\sqrt{s} = 7$ TeV [32].

carried out using the MUON spectrometer. The signal was extracted by fitting the data with a Crystal-Ball function, a technique used also for the analysis of Pb–Pb data.

The measurement of polarization in pp collisions at the LHC offers a way to further test of QCD theoretical calculations for the production mechanism of quarkonia. This may discriminate between the various QCD approaches that are not at present able to describe all quarkonia observables consistently. The right panel of Fig. 7 shows the polarization parameters λ_θ and λ_ϕ obtained from the polar and azimuthal angular distributions of the J/ψ decay muons measured at forward rapidity ($-4 < y < -2.5$) in the helicity and Collins-Soper reference frames [32]. As one can see, both λ_θ and λ_ϕ are compatible with zero in both reference frames, even if a decrease of λ_θ to ~ -0.4 in the lower p_t range is visible in the helicity reference frame.

Combining the information on the J/ψ yield in Pb–Pb collisions at $\sqrt{s_{NN}} = 2.76$ TeV in a given centrality class with that from pp collisions at the same centre-of-mass energy, it was possible to obtain the R_{AA} for J/ψ in the forward region [33]. This is shown in figure 8, where the J/ψ R_{AA} is drawn as a function of the number of participating nucleons, used as the parameter to describe the centrality of the collisions (the higher $\langle N_{part} \rangle$, the more central the event is). As one can see, the R_{AA} shows little dependence on centrality staying at the level of $\sim 0.7 \div 0.5$. Moreover, the comparison with the results from PHENIX in Au–Au collisions at $\sqrt{s_{NN}} = 0.2$ TeV [36–38], which are also reported in the figure, indicates a smaller suppression at LHC than at RHIC in central collisions. Models based on statistical hadronization, or including J/ψ regeneration from charm quarks in the QGP phase can describe the data quite well, as discussed in [33].

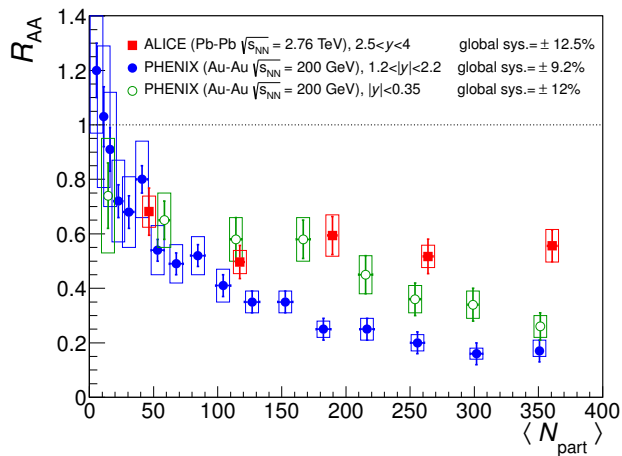


Figure 8: J/ψ R_{AA} as a function of the number of participating nucleons obtained by ALICE in Pb–Pb collisions at $\sqrt{s_{NN}} = 2.76$ TeV. The measurements by PHENIX in Au–Au collisions at $\sqrt{s_{NN}} = 0.2$ TeV are also shown [33].

5 Conclusions

The main heavy flavour results by the ALICE experiment at the LHC have been presented. The importance of the analysis of pp data has been shown in terms of QCD predictions benchmark, and as a reference for the Pb–Pb measurements. The R_{AA} of open heavy flavour exhibits a suppression of ~ 4 for D mesons in 0 – 20% centrality class events. The D meson results show an increasing suppression with centrality, seen also for electrons and muons from heavy flavour decays, which indicate that in central collisions a dense and strongly interacting medium seems to be formed. The measurement of R_{AA} of J/ψ at LHC shows a different behavior as a function of centrality compared to measurements at RHIC, which could be an indication of (re)generation of J/ψ in the QGP (or at the phase boundary).

The forthcoming p–Pb collisions foreseen for November 2012 will offer the opportunity to better understand the results of the ALICE open heavy flavour and charmonium results. They will provide key measurements to discriminate between initial and final state effects, such as shadowing, and to evaluate the degree of thermalization of open charm.

References

- [1] F. Karsch and E. Laermann, arXiv:hep-lat/0305025.
- [2] M. H. Thoma and M. Gyulassy, Nucl. Phys. **B351** (1991) 491.
E. Braaten and M. H. Thoma, Phys. Rev. **D44** (1991) 1298; Phys. Rev. **D44** (1991) 2625.
- [3] M. Gyulassy and M. Plumer, Phys. Lett. **B243** (1990) 432.
- [4] R. Baier, Y. L. Dokshitzer, A. H. Mueller, S. Peigne and D. Schiff, Nucl. Phys. **B484** (1997) 265.
- [5] Yu.L. Dokshitzer and D.E. Kharzeev, Phys. Lett. **B519** (2001) 199.
- [6] T. Matsui and H. Satz, Phys. Rev. Lett. **B178** (1986) 416.

- [7] P. Braun-Munzinger and J. Stachel, Phys. Lett. B **490** (2000) 196 [nucl-th/0007059].
- [8] R. L. Thews, M. Schroedter and J. Rafelski, Phys. Rev. C **63** (2001) 054905 [hep-ph/0007323].
- [9] B. Abelev *et al.* [ALICE Collaboration], JHEP **1207** (2012) 191 [arXiv:1205.4007 [hep-ex]].
- [10] The LHCb Collaboration, LHCb-CONF-2010-013.
- [11] The ATLAS Collaboration, ATLAS-CONF-2011-017.
- [12] C. Lourenco and H. K. Wohri, Phys. Rept. **433** (2006) 127 [hep-ph/0609101].
- [13] L. Adamczyk *et al.* [STAR Collaboration], Phys. Rev. D **85** (2012) 092010 [arXiv:1112.2980 [hep-ex]].
- [14] A. Adare *et al.* [PHENIX Collaboration], Phys. Rev. C **84** (2011) 044905 [arXiv:1005.1627 [nucl-ex]].
- [15] M. L. Mangano, P. Nason and G. Ridolfi, Nucl. Phys. B **373** (1992) 295.
- [16] A. Rossi for the ALICE Collaboration, these proceedings.
- [17] L. Manceau for the ALICE Collaboration, these proceedings.
- [18] C. Di Giglio for the ALICE Collaboration, these proceedings.
- [19] F. Carminati *et al.*, ALICE Collaboration, Physics Performance Report Vol. I, CERN/LHCC 2003-049 and J. Phys. **G30** 1517 (2003); B. Alessandro *et al.*, ALICE Collaboration, Physics Performance Report Vol. II, CERN/LHCC 2005-030 and J. Phys. **G32** 1295 (2006); K. Aamodt *et al.*, ALICE Collaboration, JINST **3** (2008) S08002.
- [20] B. Abelev *et al.* [ALICE Collaboration], JHEP **1201** (2012) 128 [arXiv:1111.1553 [hep-ex]].
- [21] M. Cacciari, M. Greco and P. Nason, JHEP **9805** (1998) 007 [arXiv:hep-ph/9803400]; M. Cacciari, S. Frixione, N. Houdeau, M. L. Mangano, P. Nason and G. Ridolfi, arXiv:1205.6344 [hep-ph].
- [22] B.A.Kniehl, G.Kramer, I.Schienbein, H.Spiesberger, in preparation.
- [23] B. Alver, M. Baker, C. Loizides, and P. Steinberg, arXiv:0805.4411; M. L. Miller, K. Reygers, S. J. Sanders, and P. Steinberg, Ann. Rev. Nucl. Part. Sci. **57**, 205 (2007).
- [24] K. Aamodt *et al.* , ALICE Collaboration, Phys. Rev. Lett **105** 252301 (2010); K. Aamodt *et al.* , ALICE Collaboration, Phys. Rev. Lett **106** 032301 (2011).
- [25] B. Abelev *et al.* [ALICE Collaboration], arXiv:1203.2160 [nucl-ex].
- [26] H. Appelshauser, J. Phys. G **38** (2011) 124014 [arXiv:1110.0638 [nucl-ex]].
- [27] R. Bailhache for the ALICE Collaboration, proceeding of the Conference *Strangeness in Quark Matter*, Cracow, Poland, 18-24 September 2011, Acta Phys. Polon. **5** Vol. 2 (2012) 291.
- [28] B. Abelev *et al.* [ALICE Collaboration], Phys. Lett. B **708** (2012) 265 [arXiv:1201.3791 [hep-ex]].
- [29] X. -N. Wang and M. Gyulassy, Phys. Rev. D **44** (1991) 3501.
- [30] X. Lopez for the ALICE Collaboration, proceeding of the Conference

Strangeness in Quark Matter, Cracow, Poland, 18-24 September 2011, Acta Phys. Polon. **5** Vol. 2 (2012) 297.

- [31] K. Aamodt *et al.* [ALICE Collaboration], Phys. Lett. B **704** (2011) 442 [arXiv:1105.0380 [hep-ex]].
- [32] B. Abelev *et al.* [ALICE Collaboration], Phys. Rev. Lett. **108** (2012) 082001 [arXiv:1111.1630 [hep-ex]].
- [33] B. Abelev *et al.* [ALICE Collaboration], arXiv:1202.1383 [hep-ex].
- [34] B. Abelev *et al.* [ALICE Collaboration], arXiv:1202.2816 [hep-ex].
- [35] B. Abelev *et al.* [ALICE Collaboration], arXiv:1203.3641 [hep-ex].
- [36] A. Adare *et al.* [PHENIX Collaboration], Phys. Rev. Lett. **98** (2007) 232301 [nucl-ex/0611020].
- [37] A. Adare *et al.* [PHENIX Collaboration], Phys. Rev. C **84** (2011) 054912 [arXiv:1103.6269 [nucl-ex]].
- [38] S. S. Adler *et al.* [PHENIX Collaboration], Phys. Rev. C **71** (2005) 034908 [Erratum-ibid. C **71** (2005) 049901] [nucl-ex/0409015].